Energy Transitions (2020) 4:113–126
https://doi.org/10.1007/s41825-020-00029-8

REVIEW

Review of solid oxide fuel cell materials: cathode, anode, and electrolyte

Saddam Hussain[1] · **Li Yangping**[1]

Received: 18 August 2020 / Accepted: 29 September 2020 / Published online: 16 October 2020

Abstract

There is a growing interest in solid oxide fuel cells (SOFCs) technology among the researchers a promising power generation with high energy efficiency, inflated fuel flexibility, and low environmental impact compared to conventional power generation systems. SOFCs are devices in which the chemical energy is directly converted into electrical energy with negligible emission. SOFCs have low pollution characteristics, high efficiency (~60%), and possess expanded fuel selection with little environmental effects. A single cell component of SOFCs is consisting an anode, cathode and an electrolyte which are stacked layer by layer to produce higher amount of power. The dense ceramic electrolyte transporting O^{2-} ions and fills the space between the electrodes material. Redox reaction occurred at the electrodes side in the presence of fuels. The operating temperatures of SOFCs of 600–1200 °C which produced heat as a byproduct and fast electro-catalytic activity while using nonprecious metals. Many ceramic materials have been investigated for SOFCs electrolyte. Yttria-stabilized zirconia (YSZ) material was extensively used as dense electrolyte in SOFCs technology. In this review, the article presents; overview of the SOFCs devices and their related materials and mostly reviewed newly available reported.

Keywords Solid electrolyte · Anode · Cathode · SOFC

Introduction

Solid oxide fuel cell (SOFC) is the technologies which are gaining more attention in the modern era due to its optimal power generation boast with enough electrical efficiency for household devices and automobiles [1–11]. Fuel cell is an energy conversion electrochemical device, which provides enormous promise for delivering substantial environmental benefits and high electrical efficiency in terms of clean and efficient electric power generation [11–16]. Among the types of fuel cells, SOFCs offer diversified advantages such as fuel flexibility, desirable energy (chemical-to-electrical) conversion efficiency that unlimited by Carnot Cycle, chemically non-pollutant, lower emission of gases, generation of heat and electricity. It is considered that SOFCs are idealistic for future clean power generation. The technology of SOFC is not limited of traditional heat engines, which admit the problems of leakage, lubrication, and heat loss [1, 17–19].

Structure and mechanism of solid oxide fuel cell

A single fuel cell consists of a cathode and an anode separated by a solid oxide electrolyte as shown in Fig. 1 [1, 5, 10–19]. The fuel (hydrogen, methane, etc.) is continuously provided to the anode side and an oxidant continuously provided to the cathode side. The fuel is decomposed into negative and positive ions at the anode terminal. The intermediate electrolyte acts as an insulator for negative ions (electrons) and allow only positive ions (protons) to flow from anode terminal to the cathode terminal. These free electrons must be recombined on the opposite side of the electrolyte membrane to become a stable system, for which the external circuits allow these free electrons move to the cathode terminal. The negative ions (electrons) generated through the oxidation of fuel at anode are accepted for oxygen reduction at cathode, which completes the external circuit. The electricity is, thus produced by the flow of electrons in the external circuit. For the real-time application, a lot of fuel cells are bunch together for the higher degree of

✉ Saddam Hussain
saddamhussain9612653@gmail.com

[1] State Key Laboratory of Solidification Processing, School of Materials Science and Engineering, Northwestern Polytechnical University, Xi'an 710072, Shaanxi, People's Republic of China

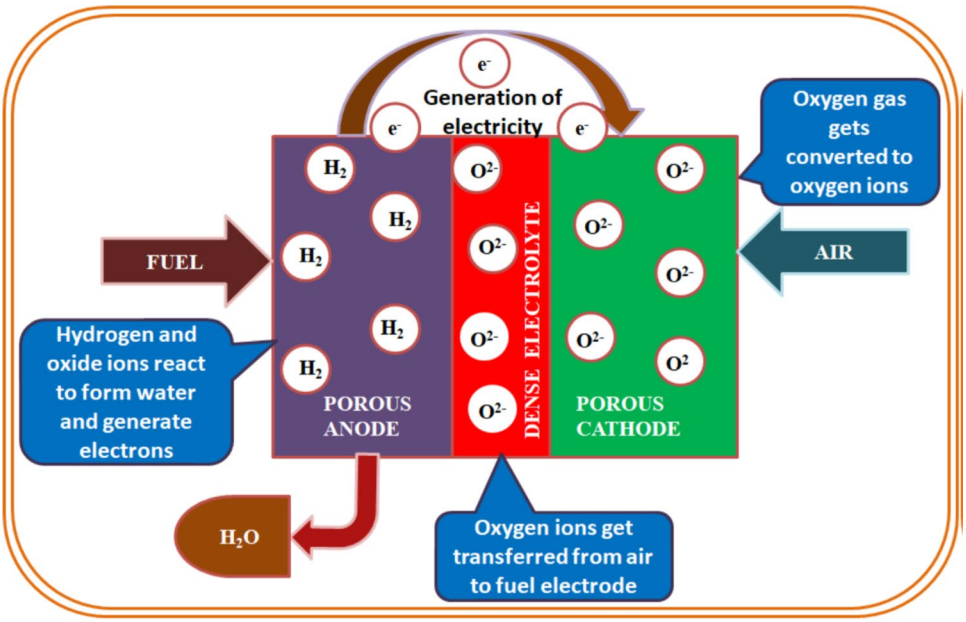

Fig. 1 Schematic diagram of solid oxide fuel cell

output power generation, while intermediate electrolyte fills up the gap between an anode and cathode transferring ions only [1–6, 16, 18].

Properties of electrolyte

The mostly electrolytes are ceramic materials which are able of conducting ions and lying between the cathode and an anode terminal. It may be proton (H^+) or an oxide ion (O^{2-}) conducting medium. The following properties for the electrolyte materials should be confirm [1–11, 20]:

1. The electrolyte materials should be higher degree of oxide, ion, or proton conductivity. A desirable conductivity is 0.01–0.1 S/cm for 1–100 µm thickness of electrolyte. If the low oxide carrying medium of the solid electrolyte, as a result prominent ohmic losses, which intending nonlinear conducting properties.
2. The electronic conductivity of the solid electrolyte should be low, while high degree of electronic conductivity results in leakage of O_2 and larger amount of voltage loss without the generating of sufficient electricity.
3. The solid electrolyte should be high enough in mechanical strength to wear efficient stress.
4. The material thermal stability is should be splendid to wearing thermal stress.
5. The solid electrolyte must have chemical, phase, dimensional, and morphological stability.
6. Low cost and easy cell fabrication technology.

Components of SOFC

During the last decade, a lot of ceramic materials have been designed to work as an electrolyte material. Among them, Yttria-stabilized zirconia (YSZ) is extensively used as solid electrolyte material in SOFC [17, 20]. Another material, Scandia-stabilized zirconia (ScSZ), has shown higher conductivity and better stability compared to YSZ [20, 21]. Scandia is an effective material in the usage of SOFCs electrolyte, but the major issues are the availability and price of Scandia [21]. Cerium Gadolinium Oxide (CGO) or Gadolinia doped Ceria (GDC) is another interesting solid electrolyte material which shows higher conductivity at low temperatures as compared to YSZ or ScSZ [20]. However, the mechanical stability, mixed ionic and electronic conduction behavior at low oxygen partial pressure, costing, and availability of Gadolinium are still the major challenges with the usage of GDC. Perovskite-based electrolyte materials is another interesting material having higher ionic conductivity at low temperature, Lanthanum Gallate ($LaGaO_3$) doped with Mg on the Ga site and Sr on the La site ($La_{1-x}Sr_x$) ($Ga_{1-y}Mg_y$) O_3 [20, 22, 23]. Several issues are related with the usage of this material such as phase stability, evaporating property of Ga at low oxygen partial pressure, mechanical stability as well as incompatibility with electrode materials, i.e., nickel oxide (NiO) which is commonly utilized as the anode material. Ni-YSZ cermet material used for anode because of the unique properties such as high order of porous in nature, high electrical conductivity, structure stability, and compatibility of thermal expansion with solid state material [17, 20,

24]. The Ni-YSZ thermal expansion coefficient (TEC) consists near to YSZ solid electrolyte as compared to Ni. This is worthy to enhance the working of Ni-YSZ based anodes and maximize the triple phase boundary (TPB) [17, 24]. Ni-YSZ-based anodes contacted with hydrocarbon fuels are related few drawbacks such as carbon deposition and contamination issues. The researchers investigated other additional materials with Ni-YSZ-based anode material to defeat the related issues and achieved higher fuel cell stability. The addition of alumina (Al_2O_3) [17, 24, 25], sliver (Ag) [25, 26], and niobium oxide (Nb_2O_5) [25, 27, 28] has been successfully investigated and modifies the Ni-YSZ cermet properties. Song et al. prepared a three-layer structured anode of Al_2O_3-YSZ, Al_2O_3-NiO, and NiO-YSZ layer [25, 29]. Al_2O_3 used with NiO to control the growth effect of NiO grains as a result to improve the electrical conduction and reduced the anode polarization. The addition of 0.2 wt% of Al_2O_3 give the most favorable results such as the electrical conductivity was achieved 1300 S/cm in a humidified hydrogen and open circuit (OC) power density of 321 W/cm^2. It is noticed worthy a significant improvement in electrical conductivity and increases 39% stability to compare the samples of without alumina. Wang et al. reported that adding alumina to Ni-YSZ cermet enhanced coking resistance and fuel cell efficiency as well [25, 30]. Using a higher amount of alumina (2.68 wt% than 0.2 wt%) reduced the electrical conductivity by 17.3% and the device stably operate at a temperature of 750 °C for 130 h. Wu et al. added silver (Ag) to Ni-YSZ cermet and studied for anode applications [26]. Anode was prepared by Co-tape casting method. Silver (Ag) was doped into anode materials while electro-less silver plating (ESP) and Ag $(NH_3)_2OH$ used as a precursor. Due to higher amount of Ag^+, was observed excellent electrochemical performance and achieved high power density. The contamination problems were controlled by the reduction of carbon fuel while utilizing hydrocarbon fuel and no effect/issue on open circuit voltage (OCV). Gd or Sm-doped ceria (CGO or CSO) and Mg-doped lanthanum gallate (LSGM) are extensively used for the applications of fuel cell systems [20, 24]. The desired thickness and ionic conductivity are responsible for the regression of the operating temperature of SOFCs based on LSGM material. The minimum operating temperature of SOFCs based on CGO or CSO and LSGM is ~ 550 °C and the desired thickness is 10 µm and ionic conductivity is 1×10^{-2} S/cm [24]. As mentioned above, YSZ shown higher electrical conductivity with high operating temperature and lasting mechanical behavior. Perovskite oxide electrodes materials containing of lanthanum, have the reacting property at high operating temperature which aims of the formation of layers ($La_2Zr_2O_7$) with high resistivity [24, 31]. LSGM-NiO composite material is less compatible for anode applications, while for perovskite based cathodes, high order of compatibility of LSGM and higher ionic conductivity with lanthanum transition oxide [24, 32]. Ceria-doped based rare earth (0.1–0.2 Sm_2O_3 or Gd_2O_3) composite has higher ionic conductivity at low operating temperature. Under the partial pressure of ~ 1×10^{-19} atm, reducing Ce^{4+} to Ce^{3+} and becomes sufficient electronic conductivity, which leads to reduce the fuel cell efficiency while operating at low temperature up to 500 °C, no more issue with electronic conductivity [24, 33].

Electrolyte materials

A ceramic material or dense layer solid oxide electrolyte was used in SOFCs which have the capacity of carrying oxygen ions and negligible or no electronic conduction to reduce the current leakage. The materials should be compatible with electrodes such as cathode and an anode and should be stable mechanically and chemically as well [10, 17]. The working mechanism of the SDCC superionic transport due to proton and ionic conductive (coexistence) phases are as shown in Fig. 2.

Sc_2O_3-ZrO_2 (ScSZ), and $BaZr_{0.8}X_{0.2}$ ($X = Y$, Gd, Sm) based electrolyte systems

Fergus et al. [34] demonstrated in his review article about the problem of low operating temperature of the zirconia-ceria-and lanthanum gallate-based electrolyte materials. YSZ is extensively used as an electrolyte in fuel cell after the stable conductive phase of ceria with fluorite cubic structure and increasing the ionic conductivity because of the increasing oxygen vacancies. ScSZ is a more beneficial conductivity than YSZ at reducing operating temperature because of the small difference in radius/size of Sc^{3+} and Zr^{4+}, forming small defect which conduct to a high concentration of mobility and compact crystal structure. Therefore, a shortcoming

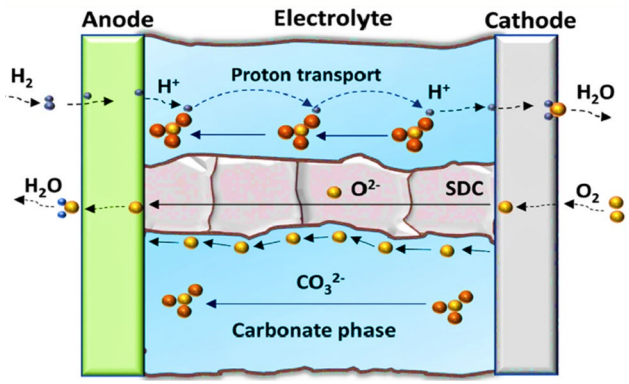

Fig. 2 Diagram of ionic & proton conductions

is also related with ScSZ is that the conductivity is equal or lower to the conductivity of YSZ below at $T = 500$ °C due to the increment in activation energy of the reduced operating temperature. In addition, a higher concentration of Scandia (typically > 8%) shows the cubic structure is transformed into rhombohedral structure and lower conductivity at lower operating temperature. Grain boundary is another important factor in IT-SOFCs because at reduced temperature the contribution of grain boundary is increase [35]. Nanostructure materials were fabricated to improve the grain boundary, which is prominently used for the applications of electrolytic materials in IT-SOFCs. Irshad et al. [36] synthesized $BaZr_{0.8}X_{0.2}O_{3-\delta}$ ($X = Y$, Sm, Gd) proton conducting perovskite structure electrolyte material by combustion route. The prepared materials (BZY, BZSm, and BZGd) were sintered at $T = 1150$ °C. The highest conductivity was found for BZY of 2.2×10^{-3} S/cm and the power density was achieved 0.34, 0.24, and 0.32 W/cm^2 for BZY, BZGd and BZSm, respectively at $T = 650$ °C.

Ceria doped-based electrolyte systems

Ceria is another doping material of fluorite structure with good ionic conductivity at low operating temperatures and low polarization resistance to comparison with zirconia [34, 37]. A major problem of ceria-doped electrolyte of electronic conduction at low oxygen (O_2) partial pressures [37]. Different ceria-doped components were investigated at low O_2 partial pressure such as $Ce_{0.8}Gd_{0.2}O_2$, $Ce_{0.9}Gd_{0.1}O_2$ (CGO) having good stability. Sm, Yb, La, and Nd doped ceria can also investigate, which shows lower conductivity than CGO [34, 38–42]. Alternating layered of nanostructured on ceria and zirconia has excellent ionic conductivities and ionic mobility [34].

LSGM-based electrolyte systems

Mn and Sr doped in $LaGaO_3$ perovskite materials to form $La_{1-x}Sr_xGa_{1-y}Mg_yO_3$ (LSGM) which is an efficient in oxygen ionic conductivity at low operating temperatures. LSGM material shows better properties at low oxygen partial pressures in comparison to CGO while its ionic conductivity is much more than that of ScSZ and YSZ [34]. Different combinations of doping were investigated and found the best ionic conductivities for $La_{0.8}Sr_{0.2}Ga_{0.8}Mg_{0.2}O_3$ and $La_{0.8}Sr_{0.2}Ga_{0.85}Mg_{0.15}O_3$ [43].

$Ce_{1-x}(Gd_{0.5}Pr_{0.5})_{xO2}$ based electrolyte systems

Ramesh et al. [44] Prepared $Ce_{1-x}(Gd_{0.5}Pr_{0.5})_xO_2$ ($x = 0.0$–0.24), a co-doped ceria ceramic electrolyte by sol–gel method at low temperature combustion. The ceramics composition $Ce_{0.84}(Gd_{0.5}Pr_{0.5})_{0.16}O_2$ was showed the highest ionic conductivity (1.059×10^{-2} S/cm) at operating temperature 500 °C. This ionic conductivity is 11.5% higher than that of GDC. Besides, for this co-doping based electrolyte, the average atomic number is 61.5 which was showed enhancement of ionic conductivity.

SDC and mixed LCP (lanthanum, cerium, and praseodymium) based electrolyte systems

Huang et al. [45] synthesized $Ce_{0.8}Sm_{0.2}O_{1.9}$ (SDC) carbonate electrolyte by oxalate coprecipitation method. The prepared SDC carbonate composite showed high ionic conductivity at low temperatures 400–600 °C and had the ability to conduct both oxygen and proton ions at similar temperatures and chemically stable, which is a more favorable feature for LT-SOFC. Zhu et al. [46] prepared mixed RE carbonates and mixed lanthanum, cerium, and praseodymium or LCP were heat treated at $T = 800$ °C for 2 h to obtain LCP-oxides.

LSCF, LSTF, and GDC based electrolyte systems

Leng et al. [47] prepared $La_{0.6}Sr_{0.4}Co_{0.2}Fe_{0.8}O_3$ (LSCF) powder by glycine nitrate combustion method. The optimal composition of LSCF-GDC (40:60 wt %) cathode with GDC electrolyte 49 μm thick film and Ni-GDC (65:35 wt %) were used anode supported SOFCs, was achieved the maximum power density of 562, 422, 257 and 139 mWcm^{-2} at operating temperatures of $T = 650$, 600, 550 and 500 °C, respectively. Ferreira et al. [48] used several processing techniques to prepare composite ionic conductors by mixing a ceria-based electrolyte and different combinations of Li and Na carbonates. The mixture of carbonates showed impressive ionic conductivity ~ 0.1 S/cm at low operating temperatures $T < 600$ °C. Francis et al. [49] prepared multilayer structure green tape by sandwiched cubic zirconia electrolyte and NiO zirconia anode material was sintered at $T \leq 1000$ °C for a few seconds under a DC electric field. A dense electrolyte with minor porosity and a layer of an anode with open porosity were produced. Zhou et al. [50] synthesized GDC and $La_{0.3}Sr_{0.7}Fe_{0.7}Ti_{0.3}O_{3-\delta}$ (LSTF) ionic semiconductor electrolyte material for the application of LT-SOFC. The GDC and LSTF ratio was 5:5 found to be the best cell performance, the power density and circuit voltage are 654 m W/cm^2 and 0.92 V, respectively, at $T = 600$ °C. The common electrolyte materials and their operating temperature as shown in Table 1.

Anode materials

Selection of anode material is a crucial regard for SOFC technology, which is depends on an electrochemical performance, microstructure, and fabrication of the cells. The

Table 1 Comparison of common electrolyte on their working temperature

Temperature			
Operational	High (800–1000 °C)	Intermediate (600–800 °C)	Low (< 600 °C)
Electrolyte	YSZ	SDC, GDC	SDCC
Descriptions	High ionic conduction (~0.1S/cm) within the operating regime The thin electrolyte is preferred to offset the ohmic resistance below ~ 800 °C	High ionic conduction (0.1 S/cm) within the operating regime Drastic performance loss at < 600 °C due to chemical & mechanical instabilities, i.e., reduction of $Ce^{4+} \rightarrow Ce^{3+}$	Superionic conductions of $H^+/O^{2-} < 600$ °C Resolve issues faced by ceria-based electrolyte The lower activation energy for charge transfer due to the existence of proton conduction H^+

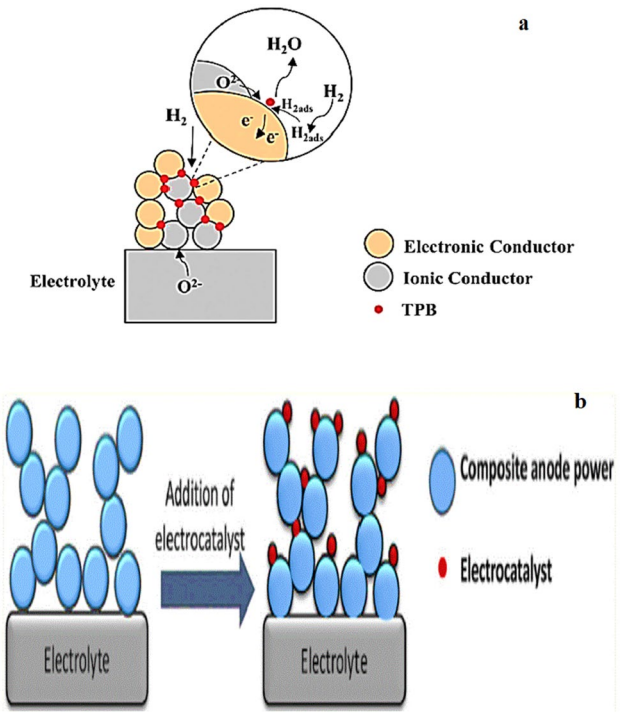

Fig. 3 **a** TPB anode material, **b** Schematic diagram of metallic electrocatalyst on anode composite substrate

desired performance of anode material should be required for two main factors. First is a large surface area of triple phase boundary help to maximize the anodic reactions. The electrochemical reaction takes place at the triple phase boundary (TPB), such as at the point of contact of electronic and oxygen ion conductor and gas as shown in Fig. 3a. Second is a prominent porous microstructure which facilitate a quickly gas transportation and reaction by product [51, 52]. Besides, anodic materials must be good in stability, high order of electronic conductivity, efficient thermally with other components of the cell, and high electro-catalytic activity. However, utilizing noble metals, have shown the extended lengths of the TPB electrodes, and the charge transfer accelerates significantly to oppress the polarisation resistance as shown in Fig. 3b. All of these factors combined to form a high-performance anode by minimizing the polarization losses.

CGO and YZT anode systems

A method was reported for the mixed ionic conductivity to determine the electrochemical properties of $Ce_{0.6}Gd_{0.4}O_{2\pm\delta}$ and $Y_{0.2}Ti_{0.18}Zr_{0.62}O_{1.9\pm\delta}$ (YZT) ceramics. The sintered electrode (YZT) polarization resistance was measured to be 0.7 Ωcm^2 at 1300 °C while the two ceramic electrodes, the polarization resistance without sintering was measured to be 0.44 and 3.7 Ωcm^2 respectively. Cowin et al. statement in his review article that, for better anode performance, the composite or cermet required the following properties such as: electro-catalytic activity for oxidation, thermal and chemical stability, high ionic and electronic conductivity, repeated redox cycles to maintain the static behavior and compatible thermal expansion co-efficient (TEC) with contacting components of cell [53].

LSCM and BCYN anode systems

It has been reported LSCM is a p-type semiconductor material with $\sigma = 1.5$ S/cm in H_2 environment and $\sigma = 38$ S/cm under ambience at $T = 900$ °C. As mentioned an above paragraph, the repetition of oxidation reduction cycles of $(La_{0.75}Sr_{0.25})\ Cr_{0.5}Mn_{0.5}O_3$ (LSCM) which conduct into the usage of interconnector $LaCrO_3$ and $La_{1-x}Sr_xMnO_3$ cathode materials [53]. LSCM composite material is an effective redox stable for both an anode and a cathode. Besides, LSCM is conductive and stable in both atmospheres such as oxidizing and reducing, and excellent performance was achieved. It was reported that the usage of LSCM composites for both electrodes is possible to construct the symmetrical SOFC with this specific property [54]. Liu et al. [55] prepared Ni exsolved Ba $(Ce_{0.9}Y_{0.1})_{0.8}Ni_{0.2}O_{3-\delta}$/GDC

novel composite anode by solution impregnation. The prepared composite shows long-term stability and good electrochemical performance in the presence of CH_4 fuel. The power density and polarization resistance were achieved to be 270 and 211 m W/cm^2 and 0.085 and 0.12 Ω cm^2 in H_2 and CH_4 fuel, respectively, at $T = 750$ °C.

Metal fluorite cermets, SCO/CFSCO, SCMO, Ni-SDC anode systems

The anode composition of $Sm_{0.2}Ce_{0.8}O_{1.9}/Co_{0.5}Fe_{0.5}$-$Sm_{0.2}Ce_{0.8}O_{1.9}$ was achieved 1200 mW/cm^2 power density at $T = 800$ °C in the presence of fuel 3% H_2O–H_2/O_2 while the cathodic material of SCF and electrolytic material of LSGM. Perovskite anode materials Sr_2CoMoO_6 (SCMO), the highest power density is 1017 mW/cm^2 for LDC, 634 mW/cm^2 for SCF and 452 mW/cm^2 for LSGM electrolytes, respectively, in the presence of H_2, wet CH_4 and dry CH_4, respectively at $T = 800$ °C for anode material Sr_2CoMoO_6 [56, 57]. The comparison of metal fluorite cermets conductivity for anode applications is reported in the review of Cowin et al. [53] The composition of anode material is 70 vol% Ni-SDC was showed the highest electronic conductivity (~ 4000 S/cm) at $T = 800$ °C with 40% H_2–N_2 of fuel.

AMZ and AMNZ anode systems

Mumtaz et al. [58] prepared $Al_{0.1}Mn_{0.1}Zn_{0.8}O$ (AMZ) and $Al_{0.1}Mn_{0.1}Ni_{0.1}Zn_{0.7}O$ (AMNZ) by solid state reaction. The crystalline sizes were found to be 52 nm and 61 nm for AMZ and AMNZ, respectively. AMZ cell volume and lattice parameters were increased because of the higher ionic size (radius) of Mn^{2+} (0.80 Å) as compared to the size of Zn^{2+} (0.74 Å). On the other hand, AMNZ cell volume and lattice parameters were decreased because of the lower ionic size (radius) of Ni^{2+} (0.69 Å) as compared to Zn^{2+} (0.74 Å). These cell volume and lattice parameters variation were the confirmation of Al and Mn successfully doped in ZnO lattice in the prepared anodic systems. However, the prepared materials both have ionic and electronic conduction, which is suitable for anode materials in LT-SOFCs.

BLITIM, BLTM anode systems

Benamira et al. [59] prepared pervoskite materials of $Ba_{0.5}La_{0.5}In_{0.3}Ti_{0.1}Mn_{0.6}O_3$ (BLITIM) and $Ba_{0.5}La_{0.5}Ti_{0.3}Mn_{0.7}O_3$ (BLTM) was showed the electronic conductivity 11.3 S/cm and 13.4 S/cm at $T = 700$ °C under the oxidative atmosphere of air, respectively. However, the above two materials conductivity decreased 0.6 S/cm and 0.3 S/cm while reducing the environment, respectively. Ni-BLITMIT/BIT07 and Ni-BLTM/BIT07-based anode materials prepared by co-sintering and tape-casting methods. Initially 40 wt% of NiO, the specific area resistance was obtained 0.11 Ωcm^2 at $T = 700$ °C which is less than Ni/BIT07 cermet. Moura et al. [60] presented in his review, porous metals such as Fe, Ag, Pt, Co, Ni, Ru, Mn group of electrodes materials are beneficial for electronic conductivity and fuel permeability for the utilization as anode materials. In these interesting groups of materials, Ni has low melting point 1453 °C and sintering temperature is 1000 °C which conducts the growth of grains in SOFC operation. Besides, Ni has poor adhesive properties on the dense electrolyte material surfaces and possesses thermal expansion coefficient (TEC) 13.3×10^{-6} K^{-1} which is contradict used with electrolytic materials of GDC (12.0×10^{-6} K^{-1}) and YSZ (10.5×10^{-6} K^{-1}).

GDC anode systems

Recently, YSZ replaced with much effective Ni-GDC nanocomposite [61] material. Chavan et al. studied the microstructure of NiO-GDC nanocomposite material, showing that decreases the activation energy with increased content of NiO. However, with low content of NiO showing that better associated network of GDC grains [61]. Changing et al. [62] also studied 65–35 wt% of NiO-GDC nanocomposite. Lanthanum strontium cobaltite ferrite (LSCF) electrode supported single cell was connected on both sides of GDC composite prepared by tape-casting method. The prepared NiO-GDC nanocomposite showing that decreased power density with decreasing temperature from 650–500 °C. Gil et al. [63] synthesized NiO-GDC 50:50 wt% nano-composite powder. To increase the TPB, with better grains connection of GDC and Ni and interconnected porous structure prepared by polymer-based complex organic solution. Chen et al. [64] investigated NiO-GDC film deposited on GDC substrate by electrostatic assisted ultrasonic spray pyrolysis technique and analyzed the parameters such as deposition temperature, electric field strength and composition. However, at 450 °C of deposition temperature were analyzed another 50:50 composition and created a number of TPB of applied voltage at 12 kV. Ding et al. prepared a single cell of LSCF nanoparticles printed over GDC-NiO-GDC by hydroxide coprecipitation method [65].

Miscellaneous anode systems

$La_{0.65}Ce_{0.1}Sr_{0.25}Cr_{0.5}Mn_{0.5}O_{3-\delta}$ (LSCM) were synthesized at 1100 °C in the presence of argon demonstrated a rhombohedral type structure, showing excellent electrochemical performance and was achieved 1.6 Ωcm^2 and 0.2 Ωcm^2 polarization resistance in wet methane and 3 wt% H_2O hydrogen at 1173 K [66]. Sinha et al. [67] were prepared the different composition of titanium oxy-carbide TiO_xC_{1-x} where $x = 0.2$–0.8 by solid state reaction at 1500 °C for

5 h. He has confirmed that titanium oxy-carbide is stable in reducing conditions and compatible with $Ce_{0.9}Gd_{0.1}O_{3-\delta}$ at intermediate operating temperature electrolytic material. Rossmeisl et al. [68] used quantum mechanical on the level of first principle calculations of density functional theory (DFT) were calculated for the surface-adsorbed stability of H_2 and O_2 atoms and hydroxyl radicals for different kinds of metals (Fe, Ni, Ru, Mn, Co, Cu, Au, Ag, Rh, Pt, Pd) which may be suitable for SOFC anodes. Yang et al. [69] synthesized $Sr_{2-x}La_xFeMoO_{6-\delta}$ ($0 \le x \le 1$) (SLFM), a type of double perovskites by solid state route and studied their performance for SOFCs as anode materials. It was observed that the crystalline symmetry of SLFM was changed from tetragonal to orthorhombic while increasing the La content which is assigned the additional electron at the antibonding orbitals of t_{2g} and e_g of Mo/Fe cations. In addition, SLFM2 has excellent electrochemical performance and the highest electrical conductivity was found in the series of SLFM due to the concentration of oxygen vacancy. Giannici et al. [70] designed an electrochemical half-cell of LSCF-YSZ for in-situ X-ray absorption spectroscopy (XAS) experiments during an electrical polarization which was investigated under the conditions of anode and cathode at 850 °C in the range of + 1 to − 1 V under applied electrical bias in air. LSCF was quickly degraded into simple oxides due to the formation of oxygen vacancy which is confirmed by XAS experiments. Verbraeken et al. [71] was synthesized $La_{0.20}Sr_{0.25}Ca_{0.45}TiO_3$ ($LSCT_{A-}$) perovskite type structure with co-doping of Ca and La at A-site by conventional solid state route. $LSCT_{A-}$ anode and LSM cathode were followed by screen printing with 160 µm thickness. Both ceria and nickel were added to improve the anode performance and reduced ohmic losses and polarization impedances. It was confirmed, after 20 redox cycles and operating at 900 °C for 250 h in humidified hydrogen (8% H_2O), showing stable redox cycling capability and specific area resistance 0.73 Ωcm^2. Steiger et al. [72] were synthesized metal oxides of $La_{0.3}Sr_{0.55}TiO_{3-\delta}$ (LST) and LSTN mixed perovskite type structure for solid oxide fuel cell anode application by citrate gel method. For the first time reported a remarkable property after sulfur poisoning, as a result preciously free metal re-generate and stable with 0.58 Ωcm^2 at 850 °C SOFC anode material. Zha et al. [73] prepared as a single-phase complex anodic material pyrochlore $Gd_2Ti_{1.4}Mo_{0.6}O_7$ by solid state reaction method which has a high catalytic performance for oxidation of containing H_2S fuel and the SOFC was regularly operated for 6 days. The specific area resistance was 0.2 Ωcm^2 at 950 °C and the maximum power density is 342 Wcm^2 under the mixture of fuel gas (H_2S: H_2 = 10%:90%). Li et al. [74] were successfully synthesized NiO-YSZ ceramic anode material by dry-pressing method with different concentration of Bi_2O_3. It is found that after investigation, increasing the concentration of Bi_2O_3, reduce sintering temperature and increased relative density, weight loss, and bending strength. However, an addition of 6 wt% of Bi_2O_3, observed the sintering temperature was reduced to 1250 °C and no effect on the phase composition and conductivity. Dong et al. [75] was successfully synthesized Sn doped double perovskite $PrBaFe_{(2-x)}Sn_xO_{5+\delta}$ (x = 0–0.3) anodic material by a combustion method. It is found that different crystal structures which are depending on the doping level of Sn and good stability in dual atmosphere (reducing and redox). Shaheen et al. [76] synthesized $Cu_{0.5}Sr_{0.5}$ (CS) and $La_{0.2}Cu_{0.4}Sr_{0.4}$ (LCS) mixed metal oxide nanocomposites by Pechini method. The porous structure and crystallinity of the prepared nanocomposite enhanced the electrochemical performance. The maximum power density of 725 and 782 m W/cm^2 for CS and LCS, respectively, at T = 600 °C.

Cathode materials

Perovskite structure cathode systems

ABO_3 perovskite structure having unique properties and integrated with A- and B-cations. Alkali metals, rare-earth metals, alkaline earth metals, elements of 6th period, and group 13–15 cations are usually belonging to A-site. The perovskite cubic close-packing structure formed by large A- cations due to the comparable size of O^{2-} ion and octahedral voids (1/4 parts) occupied by B- cations. The electronic properties of perovskite material are possibly to alter because of the order of distortion and due to partially replacement in the sub-lattices of both A- and B-cations. The interaction between 2*p*-orbitals of oxygen and d-orbitals of transition metal which conducts to the formation of wide energy bands. The distorted structure of perovskite, the bands remain narrows and shows dielectric properties as well as in localization of electronic state due to rotation of octahedra. The conductivity of the perovskite depends on the structure distortion, for example; doping of rare earth ions in perovskite which leads to increase the distortion due to the radius of rare earth metal cation decreases. The temperature of transition-to-metal was typically increased from 135 in Pr to 403 K in Sm, which means the large radius of rare earth metal cations such as La, Ce, and Pr possesses the highest conductivity in RBO_3 perovskite. The selection of perovskite type cathodic material based on transition metal oxide in the variation of oxidation state. The higher oxidation states increase from 3 to 4d and 5d in the row of periodic table, which means that higher conductivity cations of 4d and 5d in lower oxidation states such as niobium while 3d elements such as $LaTiO_3$ are not stable in the oxidative environment of cathode gases. $LaMO_3$ perovskite-type transition metal oxide where M = Mn, Cr, Co, Ni, and Fe of p-type conductivity is stable in the oxidation atmosphere in a certain

range of temperature [77]. To enhanced the conductivity by increasing the charge carrier (hole concentration) due to the substitution of heterovalent La^{3+} with Sr^{2+}, Ca^{2+} or Ba^{2+}.

Thermal expansion co-efficient (TEC) is another important parameter for cathodic material in SOFC technology, which should be matched the other components of fuel cell and directly related to the asymmetric behavior of the interatomic potential. Due to the thermal heating, the equilibrium position of atoms is displaced and shows anharmonic behavior. The thermal expansion coefficient depends on the electronic or ferroelectric magnetic properties and chemical composition as well in perovskite type oxide with an increase in temperature. An increasing temperature is directly related to the increment in oxygen vacancies, which decreases the transition metal oxide of oxidation state and typically the enhancement of metal–oxygen bonds. Besides, thermal expansion co-efficient also depends on thermally activated transitions of different states of spin such as $LaCoO_3$ is higher thermal expansion co-efficient in contrast to $LaFeO_3$ or $LaNiO_3$. However, high thermal expansion coefficient is caused by spin transitions between the high ($t_{2g}^4 e_g^2$) states and low-spin ($t_{2g}^6 e_g^0$) stated of cobalt (Co^{3+}) cation [77, 78]. The main shortcoming of cobalt (Co)-perovskite is the high TEC with related transformations between the low-and high-spin-induced states of Co^{3+} cation. Besides, Cobalt (Co)-perovskites material is highly reactive with the electrolytes of YSZ-based. To avoid/reduce this drawback/reactivity, a protective layer of GDC can be deposited between the YSZ electrolyte and cathode material, the deposited GDC layer is inert with respect to cobalt (Co)-oxide at the temperature of deposition. However, too many complexities come up during the long-term operation of SOFC because of the actions of diffusion via the GDC layer. In addition, another method is also used to control this drawback, cobalt is partially replace by another B-site cation such as Mn, Ni, Fe, or Cu [79]. For example, $La_{1-x}Sr_xCoO_{3-\delta}$ composite was found high conductivity (> 100 S/cm) and TEC (15.4 ppm/K) at 800 °C operating temperature of fuel cell with high order of catalytic activity and highly O_2 self-diffusion co-efficient [77].

NBCO cathode systems

$NdBa_{1-x}Co_2O_{5+\delta}$ ($NB_{1-x}CO$, $x = 0.00$–0.06) were synthesized have tetragonal layer pervoskite structure for cathodic material. Besides, the O_2 vacancy is raised with the increasing concentration of Ba deficiency, while the thermal expansion coefficient was found to decrease with the increasing of Ba deficiency. The result was suggested that lower polarization resistance and release of lattice oxygen by the introduction of Ba deficiency. Among all the prepared samples, $NB_{0.96}CO$ oxide is more enough porosity and appropriate grain size, which is established as a potential cathodic material for IT-SOFCs technology [80].

Co-doped PBSCFO cathode systems

$LnBa_{0.5}Sr_{0.5}Co_{2-x}Fe_xO_{5+\delta}$ (LnBSCF), where Ln = Pr and Nd; $x = 0$, 0.25, 0.5, 0.75 and 1.0 or co-doped PBSCFO were synthesized by glycine nitrate process (GNP) for low temperature SOFCs. Fast ionic diffusions were found through pore channels and high degree of catalytic activity at low temperatures, having good stability and splendid compatibility with electrolyte materials under the FCs operating conditions [81]. Ma et al. [82] synthesized ceramic oxides of $La_{0.5-x}Pr_xSr_{0.5}FeO_{3-\delta}$ ($x = 0$, 0.25, 0.5) by wet chemical route. Pr has hydration ability and the oxide hydration energy was decreased with the increasing concentration of Pr.

SDC cathode systems

The SDC ($Sm_{0.2}Ce_{0.8}O_{1.8}$), Sm-doped ceria used as electrolyte, and $Sm_{0.5}Sr_{0.5}CoO_3$ (SSC) were used as porous cathodes in the fabrication of fuel cell. The thickness of SDC electrolyte is about ~ 25 µm and NiO-SDC was used as an anode by co-pressing technique to form a bilayer structure. The microstructure of cathode materials, electro-chemical properties, and type of composition were studied. Besides, the effect of firing temperature were also studied and 950 °C firing temperature was more suitable for the application of SDC cathodic systems. An appropriated selection of SDC: SSC ratios was shown enhanced the catalytic performance. Dai et al. [83] added Co in SDC and successfully prepared $Sm_{0.5}Sr_{0.5}CoO_{3-\delta}$ (SSC) powder for the cathodic application. The cell was sintered at $T = 1000$ °C showed excellent performance, desirable polarization, and ohmic resistance.

La (Sr) FeO3 and Co-based cathode systems

Baumann et al. [84] were synthesized two materials, $Ba_{0.5}Sr_{0.5}Co_{0.8}Fe_{0.2}O_{3-\delta}$ (BSCF) and $(La_{0.6}Sr_{0.4})_{0.9}Co_{0.8}Fe_{0.2}O_{3-\delta}$ (LS09CF) by Pechini method. Using pulsed laser deposition (PLD) method was used for thin films of the prepared materials. The substitution at A-site of La in this material by Sm conducts effective improvement of the surface exchange kinetics, especially by the substitution of Ba. A little effect was observed on the surface exchange kinetics while changing the ratio of Co/Fe between 0 and 1 at around 750 °C. The electrochemical activation effect was also investigated for different materials, i.e., catalytic activity in regards O_2 surface interchange by dc bias treatment.

Triple-conducting oxide layer-based ($H^+/O^{2-}/e^-$) cathode systems

Kim et al. [85] were prepared $NdBa_0Sr_{0.5}Co_{1.5}Fe_{0.5}O_{5+\delta}$ (NBSCF) by Pechini method. The synthesized materials high degree of stability over 500 h at 1023 K with excellent power density 1.61 W/cm^2. Triple conducting oxides (TCOs) are the intrinsic ability to increase the electrochemical activity between the electrolyte and cathode. The triple-conducting oxide ($H^+/O^{2-}/e^-$) cathode NBSCF have good compatibility with respect to proton-conducting electrolyte barium/zirconium/cerium/yttrium/ytterbium (BZCYYb) is an effective candidate for IT-SOFC applications.

$SrCo_{0.9}Nb_{0.1}O_{3-\delta}$ (SCN)-based cathode systems

Wang et al. [86] synthesized a new liquid phase for the formation of Nb ceramic of $SrCo_{0.9}Nb_{0.1}O_{3-\delta}$ (SCN), which is offering the lower reaction temperature for the phase formation and smaller particle size as well. These SCN cathodes are suitable materials for the proton conducting applications. Besides, $BaCe_{0.4}Zr_{0.4}Y_{0.2}O_{3-\delta}$ (BCZY442) electrolyte was employed with these SCN cathodes to formed proton-conducting SOFC which showed the maximum power density of 348 mW/cm^2 at the operating temperature of 700 °C. The SCN cathode was also prepared by solid state reaction (SSR) at the same temperature with a maximum power density of 204 mW/cm^2, which is much lower in comparison with a new liquid phase SCN cathode.

Cobalt-free cathode systems

Co-containing cathodes are well known ability to operate at high temperature in SOFCs technology. To reduce the operating temperature from the range of intermediate temperature-to-low temperature may conduct to a mismatch in the TEC. Co-free cathodes were the best alternative way for the higher electrochemical efficiency cells in the range of intermediate temperature-to-low temperature (IT-LT) [87]. Ding et al. [88] prepared $GdBaFe_2O_{5+\delta}$ (GBF), a promising perovskite Co-free cathode for IT-SOFC by Pechini method which shows good catalytic activity. Lee et al. [89] synthesized Co-free Ca_2Fe_2O-$Ce_{0.9}Gd_{0.1}O_{1.95}$ (CFO)-(GDC) composite by citrate combustion process. The mixing of GDC and $Ca_2Fe_2O_5$ particles to reduce the TEC values. Co-free $SrFe_{0.9}Nb_{0.1}O_{3-\delta}$ (SFN) cubic perovskite oxide was prepared by solid state reaction in which the dopant elements can be added to A-sites or B-sites. The maximum power density was achieved 407 mW/cm^2 at 800 °C [90]. Jiang et al. also prepared Co-free SNF cathode material which is followed by two-stage calcination to produce good quality powders, which showed the overall performance is enhanced. The single cell was achieved the maximum power density of 1403 mW/cm^2 at similar temperature which is much higher to the previous report [91]. Yu et al. [92] prepared $SrFe_{1-x}Ti_xO_{3-\delta}$ (SFT, $x=0.00$–0.15) oxides by solid state reaction. Conventional method (SSR) compared with double-stage calcination process, combustion method is more efficient for the production of cobalt-free cathodes. Ling et al. [93] synthesized Co-free cubic perovskite oxide $Sm_{0.5}Sr_{0.5}Fe_{0.8}Cu_{0.2}O_{3-\delta}$ (SSFCu) by combustion method. The TEC value of SSFCu was an approach to the SDC electrolyte material. Oxygen (O_2) vacancies are increases which enhanced the electrochemical performance because of the addition of Cu^{3+} at B-cations. Zhu et al. [94] synthesized $Sm_{0.6}Sr_{0.4}FeO_{3-\delta}$ (SSF) by combustion method and mixing of $Ce_{0.8}Cm_{0.2}O_{2-\delta}$ (SDC) electrolyte composite for enhancing the mismatch of TPB and TEC. In perovskite structure, materials, Mo, Ti, and Cu-substituted cobalt at B-cations showed the polarization resistance between of 0.05–0.250 Ωcm^2, which is excellent performance in comparison to cobalt-enhanced cathodic material.

Miscellaneous cathode systems

Duan et al. [95] prepared Y and Zr co-doped $BaCo_{0.4}Fe_{0.4}Zr_{0.1}Y_{0.1}O_{3-\delta}$ (BCFZY0.1) perovskite structure for protonic ceramic fuel cell (PCFCs) and it is applied for Lt-SOFCs. It shows high O_2 reduction reaction activity, long-term stability, and lower order of activation energy, low temperature response, large lattice parameter, and excellent compatibility with Ce-based SOFC electrolytes. The prepared cathode material showed peak power density of 0.97 W/cm^2 at 500 °C an operating temperature with 2500 h stable response and without any degradation performance after more than 80 immediate repeated cycles of ramping temperature. Besides, a peak power density was reached 0.13 W/cm^2 while an operating temperature at 350 °C and indicates beneficial CO_2 and H_2O tolerance. Zhang et al. [96] synthesized $SrFeO_{3-\sigma-\delta}F_\sigma$ (SFF_σ, $\sigma=0$, 0.05, and 0.10) and $SrFe_{0.9}Ti_{0.1}O_{3-\sigma-\delta}F_\sigma$ ($SFTF_\sigma$, $\sigma=0$, 0.05 and 0.10) perovskite oxy-fluorides by sol–gel method using a combined EDTA-CA (ethylenediaminetetra-acetic acid-citric acid) to improve the electrochemical performance. Due to an appropriate amount of anion doping, induced surface exchange properties hold sufficient stability and enhanced O_2 reduction reaction activity, such activity assigned to improved bulk diffusion at intermediate temperature. The prepared perovskite oxy-fluorides show high catalytic activity and attaining the values of an area specific resistance is 0.875, 0.393, and 0.491 Ωcm^2 for $SrFeO_{3-\delta}$, $SrFeO_{2.95-\delta}F_{0.05}$ and $SrFeO_{2.90-\delta}F_{0.10,}$ respectively at $T=600$ °C in air. Li et al. prepared Ta and Nb co-doped $SrCo_{0.8}Nb_{0.1}Ta_{0.1}O_{3-\delta}$ (SCNT) perovskite material by solid state reaction for cathodic application. The area-specific resistances are ~ 0.16 and ~ 0.68 Ωcm^2 with a peak power density of 1.2 and 0.7 W/cm^2 at

$T = 500$ and 450 °C, respectively, for an anode supported GDC based symmetrical fuel cell. Doping of Nb and Ta allows for interactive environment by inducing surface electron transfer, desirable ionic mobility, and O2 vacancies at $T \leq 500$ °C [97, 98]. Hussain et al. [99] synthesized $La_xSr_{1-x}Fe_{1-y}Cu_yO_{3-\delta}$ ($x = 0.54$, 0.5, $y = 0.2$, 0.4) perovskite structure by sol–gel method. $La_{0.54}Sr_{0.46}Fe_{0.80}Cu_{0.20}O_{3-\delta}$ composition were showed excellent performance and good conductivity among other prepared compositions. The maximum power density was achieved of 452 mW/cm^2 and the maximum conductivity was 9.029 S/cm at $T = 600$ °C.

Nanomaterials for SOFCs

The nanoscience and nanotechnology play a key role to resolve many issues because of the modification of properties in SOFCs. Recently, researchers focus on methods and materials to prepare an excellent performance of nanostructures SOFCs. Nanosize of materials has unique properties for enhancing grain boundary ionic conductivity of electrolytes in SOFCs devices. Arico et al. [100] reported in his review on nanostructured materials for energy storage devices, the development of low operating temperature FCs (< 200 °C), fuel reforming and hydrogen (H_2) storage technology, the development and dispersion of nonprecious and precious nonmetallic and metallic catalysts, and manufacturing of membrane electrode assemblies (MEA). Nanosized powders of ceria-based such as CGO, YDC, SDC, and YSZ (8% Y_2O_3-ZrO_2) induced the reduction of firing temperature in the fabrication of cells because of the different sintering properties of those polycrystalline powders. In addition, the mixed ionic and electronic conduction properties of nanosized Ce optimized the charge transfer reactions at the interface of electrodes and electrolyte. Point defects are heady for originating the ionic charge carrier in these electro-ceramic materials. Nanostructured based systems, larger surface area and grain boundaries facilitate an enhanced the number of mobile defects in the region of space charge which is entirely differ electrochemical behavior in comparison of bulk materials. Yuan et al. [101] focused on the preparation of Ce-based and controlled synthesis nanomaterials, crystal plan orientation, particle size, and tailor shape, and assembling them in an effective way. Different methods were used for synthesis such as solvothermal synthesis, CeO_2–ZrO_2 nanomaterials by solid state solution method, RE ion doped $Ce_xZr_{1-x-y}RE_yO_{2-z}$ solid solution nanomaterials, hydrolysis process $Ce_{1-x}Zr_xO_2$ solid solution for nanostructured. Dong et al. [102] synthesized a nanosized electrolyte material of $Ce_{0.8}Gd_{0.2}O_{2-\delta}$ and $Ce_{0.79}Gd_{0.2}Cu_{0.01}O_{2-\delta}$ by polyvinyl alcohol-assisted combustion method which is cubic fluorite crystalline structure and porous foamy morphology. Bellino et al. [103] prepared a cobaltite nanotube cathode of $La_{0.6}Sr_{0.4}CoO_3$ showing low polarization resistance and high porosity. Martinelli et al. [104] synthesized nanoparticles of $La_{0.8}Sr_{0.2}MnO_3$ cathode and investigated the effect of agglomeration and the variation of particle size in SOFCs. Zhi et al. [105] synthesized LSCF nanofibers by electro-spinning process for the applications of cathode in IT-SOFCs with YSZ electrolyte. Additional doping of 20 wt% GDC to enhance the power density of 1.07 W/cm^2 at operating temperature 750 °C. The 3D nanofiber cathodic network has various advantages such as (1) high percolation (2) high porosity (3) continuously charge transportation (4) excellent thermal stability under the similar operating temperature. Ishihara et al. [106] introduced the nanosized materials in his review article for the application of electrodes in IT-SOFCs. A nanosized columnar morphology (vertically aligned or double columnar) deposited by pulsed laser ablation method for improving the performance of cathodic materials and can be achieved more power density or stability by controlling the interface or the electrode structure at the scale of nanolevel. Yoon et al. [107] deposited a thin film of vertically aligned nanocomposite (VAN) structured between the GDC electrolyte and the thin layer of $La_{0.5}Sr_{0.5}CoO_3$ (LSCO) cathode was achieved higher efficiency of thin-film SOFCs. The deposited layer showed a unique characteristic improving the TPB (by ~ 14–25 times) and lower polarization resistance between the electrolyte/cathode interfaces. Evans et al. [108] prepared a cathode by spin-coating suspension nanoparticles of $La_{0.6}Sr_{0.4}CoO_{3-\delta}$ (LSC) followed by salt-assisted spray pyrolysis. A 3d porous microstructure exhibit 250 nm thin and having around 45 nm of grain size can be integrable onto free-standing electrolyte membranes of 3 mol% YSZ (3YSZ). Guan et al. [109] successfully investigated a 3D porous type of microstructure of Ni-YSZ anode material by X-ray nano-tomography. Boldrin et al. [110] produced SOFCs anodic material with $NiNO_3$ (nickel nitrate) solution by impregnating GDC scaffolds. These scaffolds were prepared utilizing inks containing of commercial GDC, a mixture of GDC nanoparticles and polymeric pore formers. In the heat treated, these scaffolds are showed better performance at low operating temperature (< 700 °C) in H_2 and excellent performance at all temperatures utilizing syngas with maximum power density 0.15 W/cm^2 at T = 800 °C. Pelegrini et al. [111] reported in his review article nanostructured Ni/Cu-YSZ material from nano-powders to improve the TPB region for anodic applications in SOFCs. Kwon et al. [112] reported Co–Ni alloy nanoparticles and synthesized $PrBaMn_{1.7}Co_{0.1}Ni_{0.2}O_{5+\delta,}$ a double layered perovskite by Pechini method. These alloy nanoparticles have better catalytic activity in FCs. Density functional theory (DFT) calculations used for better understanding of the formation of alloy nanoparticles. The free Gibbs energy of the formation of surface alloy is more desirable in comparison with bulk surface alloy formation. Cavallaro

et al. [113] investigated $La_{0.8}Sr_{0.2}CoO_{3-\delta}$ dense films was deposited at various temperatures by pulsed laser deposition on Silicon (Si) substrate for the applications of cathodic material. Depending on the different deposition temperature, amorphous or textured polycrystalline film were obtained. It was observed O_2 diffusion co-efficient had occurred an amorphous film which is four times more in comparison in crystalline materials and associated improvement of the surface exchange coefficient.

Conclusion

SOFCs has been studied across worldwide because of the fuel flexibility and actual power generation devices with low environmental impact. In this review article, to summarized both types of SOFCs electrodes such as cathode and anode and their importance in SOFCs technology. It has been reviewed that nanomaterials easily enhanced the performance of SOFCs devices. There is much more attention need to develop a higher performance of nanostructure materials which can be operated at low temperature. This will increase the importance of SOFCs technology. However, cost reduction is still a key problem in SOFCs technology.

References

1. Irshad, M., Siraj, K., Raza, R., Ali, A., Tiwari, P., Zhu, B., Rafique, A., Ali, A., Kaleem Ullah, M., Usman, A.: A brief description of high temperature solid oxide fuel cell's operation, materials, design, fabrication technologies and performance. Sci. Appl. (2016). https://doi.org/10.3390/app6030075
2. Dziurdzia, B., Magonski, Z., Jankowski, H.: Commercialisation of solid oxide fuel cells—opportunities and forecasts. IOP Conf. Ser. Mater. Sci. Eng. (2016). https://doi.org/10.1088/1757-899X/104/1/012020
3. Ruiz-Morales, J.C., Canales-Vázquez, J., Savaniu, C., Marrero-López, D., Zhou, W., Irvine, J.T.S.: Disruption of extended defects in solid oxide fuel cell anodes for methane oxidation. Nature **439**, 568–571 (2006). https://doi.org/10.1038/nature04438
4. Muecke, U.P., Beckel, D., Bernard, A., Hutter, A.B., Graf, S., Infortuna, A., Muller, P., Rupp, J.L.M., Schmeider, J., Gauckler, L.J.: Micro solid oxide fuel cells on glass ceramic substrates. Adv. Funct. Mater. **18**, 3158–3168 (2008). https://doi.org/10.1002/adfm.200700505
5. Saebea, D., Authayanun, S., Patcharavorachot, Y.: Performance evaluation of low-temperature solid oxide fuel cells with SDC-based electrolyte. Chem. Eng. Trans. **52**, 223–228 (2016). https://doi.org/10.3303/CET1652038
6. Wang, W., Su, C., Wu, Y., Ran, R., Shao, Z.: Progress in solid oxide fuel cells with nickel-based anodes operating on methane and related fuels. Chem. Rev. **113**, 8104–8151 (2013). https://doi.org/10.1021/cr300491e
7. Zuo, C., Liu, M., Liu, M.: Solid oxide fuel cells. Conv. Altern. Energy Sol-Gel Process (2012). https://doi.org/10.1007/978-1-4614-1957-0_2
8. Futamura, S., Muramoto, A., Tacjikawa, Y., Matsuda, J., Lyth, S.M., Shiratori, Y., Taniguchi, S., Sasaki, K.: SOFC anodes impregnated with noble metal catalyst nanoparticles for high fuel utilization. Int. J. Hydrogen Energy **44**, 8502–8518 (2019). https://doi.org/10.1016/j.ijhydene.2019.01.223
9. Laguna-bercero, M.A., Raimond, P., Campana, R., Larra, A.: SOFC cathodic layers using wet powder spraying technique with self synthesized nanopowders. Int. J. Hydrogen Energy **44**, 7555–7563 (2019). https://doi.org/10.1016/j.ijhydene.2019.01.220
10. Chelmehsara, M.E., Mahmoudimehr, J.: Techno-economic comparison of anode-supported, cathode-supported, and electrolyte-supported SOFCs. Int. J. Hydrogen Energy **43**, 15521–15530 (2018). https://doi.org/10.1016/j.ijhydene.2018.06.114
11. Wilson, J.R., Kobsiriphat, W., Mendoza, R., Yi Chen, H., Hiller, J.M., Miller, D.J., Thornton, K., Voorhees, P.W., Adler, S.B., Barnett, S.A.: Three-dimensional reconstruction of a solid-oxide fuel-cell anode. Nat. Mater. **5**, 541–544 (2006). https://doi.org/10.1038/nmat1668
12. Papandrew, A.B., Chisholm, C.R.I., Elgammal, R.A., Özer, M.M., Zecevic, S.K.: Advanced electrodes for solid acid fuel cells by platinum deposition on CsH_2PO_4. Chem. Mater. **23**, 1659–1667 (2011). https://doi.org/10.1021/cm101147y
13. Bessler, W.G., Vogler, M., Stormer, H., Gerthsen, D., Utz, A., Weber, A., Tiffee, E.I.: Model anodes and anode models for understanding the mechanism of hydrogen oxidation in solid oxide fuel cells. Phys. Chem. Chem. Phys. **12**, 13888–13903 (2010). https://doi.org/10.1039/c0cp00541j
14. Lohmann, F.P., Schulze, P.S.C., Wagner, M., Naumov, O., Lotnyk, A., Abel, B., Varga, A.: The next generation solid acid fuel cell electrodes: stable, high performance with minimized catalyst loading. J. Mater. Chem. A **5**, 15021–15025 (2017). https://doi.org/10.1039/c7ta03690f
15. Walkowiak-kulikowska, J.: Polymers application in proton exchange membranes for fuel cells (PEMFCs). Phys. Sci. Rev. **8**, 1–34 (2017). https://doi.org/10.1515/psr-2017-0018
16. Salameh, Z.: Energy storage-4. Renew. Energy Storage (2014). https://doi.org/10.1016/B978-0-12-374991-8.00004-0
17. Mahato, N., Banerjee, A., Gupta, A., Omar, S., Balani, K.: Progress in material selection for solid oxide fuel cell technology: a review. Prog. Mater. Sci. **72**, 141–337 (2015). https://doi.org/10.1016/j.pmatsci.2015.01.001
18. Han, F., Mucke, R., Gestel, T.V., Leonide, A., Menzler, N.H., Buchkremer, H.P., Stover, D.: Novel high-performance solid oxide fuel cells with bulk ionic conductance dominated thin-film electrolytes. J. Power Sources **218**, 157–162 (2012). https://doi.org/10.1016/j.jpowsour.2012.06.087
19. Ma, Y., Wang, X., Zhu, B., Muhammed, M.: Microwave synthesis of mesoporous Cu-$Ce_{0.8}Sm_{0.2}O_{2-\delta}$ composite anode for low-temperature ceramic fuel cells. Int. J. Hydrogen Energy **38**, 597–602 (2012). https://doi.org/10.1016/j.ijhydene.2012.07.018
20. Laosiripojana, N., Wiyaratn, W., Kiatkittipong, W., Arpornwichanop, A., Soottitantawat, A., Assabumrungrat, S.: Reviews on

solid oxide fuel cell technology. Eng. J. **13**, 65–83 (2009). https://doi.org/10.4186/ej.2009.13.1.65
21. Basu, R.N.: Materials for solid oxide fuel cells. Recent Trends Fuel Cell Sci. Technol. (2007). https://doi.org/10.1007/978-0-387-68815-2_12
22. Gong, W., Gopalan, S., Pal, U.B.: Performance of intermediate temperature (600–800 °C) solid oxide fuel cell based on Sr and Mg doped lanthanum-gallate electrolyte. J. Power Sources **160**, 305–315 (2006). https://doi.org/10.1016/j.jpowsour.2006.01.039
23. Jiang, S.P.: Development of lanthanum strontium cobalt ferrite perovskite electrodes of solid oxide fuel cells–a review. Int. J. Hydrogen Energy **44**, 7448–7493 (2019). https://doi.org/10.1016/j.ijhydene.2019.01.212
24. Jacobson, A.J.: Materials for solid oxide fuel cells. Chem. Mater. **22**, 660–674 (2010). https://doi.org/10.1021/cm902640j
25. da Silva, F.S., de Souza, T.M.: Novel materials for solid oxide fuel cell technologies: a literature review. Int. J. Hydrogen Energy **42**, 26020–26036 (2017). https://doi.org/10.1016/j.ijhydene.2017.08.105
26. Tian, X.Y., Zhang, J., Zuo, W., Kong, X., Wang, J., Sun, K., Zhou, X.: Enhanced electrochemical performance and carbon anti-coking ability of solid oxide fuel cells with silver modified nickel-yttrium stabilized zirconia anode by electroless plating. J. Power Sources **301**, 143–150 (2016). https://doi.org/10.1016/j.jpowsour.2015.10.006
27. Choi, S., Wang, J., Cheng, Z., Liu, M.: Surface modification of Ni-YSZ using niobium oxide for sulfur-tolerant anodes in solid oxide fuel cells. J. Electrochem. Soc. **155**, B449 (2008). https://doi.org/10.1149/1.2844366
28. Ding, H., Tao, Z., Liu, S., Yang, Y.: A redox-stable direct-methane solid oxide fuel cell (SOFC) with $Sr_2FeNb_{0.2}Mo_{0.8}O_{6-\delta}$ double perovskite as anode material. J. Power Sources **327**, 573–579 (2016). https://doi.org/10.1016/j.jpowsour.2016.07.101
29. Song, X., Dong, X., Li, M., Wang, H.: Effects of adding alumina to the nickel-zirconia anode materials for solid oxide fuel cells and a two-step sintering method for half-cells. J. Power Sources **308**, 58–64 (2016). https://doi.org/10.1016/j.jpowsour.2016.01.070
30. Wang, F., Wang, W., Ran, R., Tade, M.O., Shao, Z.: Aluminum oxide as a dual-functional modifier of Ni-based anodes of solid oxide fuel cells for operation on simulated biogas. J. Power Sources **268**, 787–793 (2014). https://doi.org/10.1016/j.jpowsour.2014.06.087
31. Shu, L., Sunarso, J., Hashim, S.S., Mao, J., Zhou, W., Liang, F.: Advanced perovskite anodes for solid oxide fuel cells: a review. Int. J. Hydrogen Energy **44**, 31275–31304 (2019). https://doi.org/10.1016/j.ijhydene.2019.09.220
32. Kaur, P., Singh, K.: Review of perovskite-structure related cathode materials for solid oxide fuel cells. Ceram. Int. **46**, 5521–5535 (2020). https://doi.org/10.1016/j.ceramint.2019.11.066
33. Fan, L., Wang, C., Chen, M., Zhu, B.: Recent development of ceria-based (nano) composite materials for low temperature ceramic fuel cells and electrolyte-free fuel cells. J. Power Sources **234**, 154–174 (2013). https://doi.org/10.1016/j.jpowsour.2013.01.138
34. Fergus, J.W.: Electrolytes for solid oxide fuel cells. J. Power Sources **162**, 30–40 (2006). https://doi.org/10.1016/j.jpowsour.2006.06.062
35. Guo, X., Waser, R.: Electrical properties of the grain boundaries of oxygen ion conductors: acceptor-doped zirconia and ceria. Prog. Mater. Sci. **51**, 151–210 (2006). https://doi.org/10.1016/j.pmatsci.2005.07.001
36. Irshad, M., Ain, Q.U., Siraj, K., Raza, R., Tabish, A.N., Rafique, M., Idrees, R., Khan, F., Majeed, S., Ahsan, M.: Evaluation of BaZr0.8X0.2 (X=Y, Gd, Sm) proton conducting electrolytes sintered at low temperature for IT-SOFC synthesized by cost effective combustion method. J. Alloys Compd. (2020). https://doi.org/10.1016/j.jallcom.2019.152389
37. Dalslet, B., Blennow, P., Hendriksen, P.V., Bonanos, N., Lybye, D., Mogensen, M.: Assessment of doped ceria as electrolyte. J. Solid State Electrochem. **10**, 547–561 (2006). https://doi.org/10.1007/s10008-006-0135-x
38. Park, J.Y., Yoon, H., Wachsman, E.D.: Fabrication and characterization of high-conductivity bilayer electrolytes for intermediate-temperature solid oxide fuel cells. J. Am. Ceram. Soc. **88**, 2402–2408 (2005). https://doi.org/10.1111/j.1551-2916.2005.00475.x
39. Sameshima, S., Hirata, Y., Ehira, Y.: Structural change in Sm- and Nd-doped ceria under a low oxygen partial pressure. J. Alloys Compd. **408–412**, 628–631 (2006). https://doi.org/10.1016/j.jallcom.2004.12.072
40. Hartmanová, M., Lomonova, E.E., Navrátil, V., Šutta, P., Kundracik, F.: Characterization of yttria-doped ceria prepared by directional crystallization. J. Mater. Sci. **40**, 5679–5683 (2005). https://doi.org/10.1007/s10853-005-2795-9
41. Suda, E., Pacaud, B., Mori, M.: Sintering characteristics, electrical conductivity and thermal properties of La-doped ceria powders. J. Alloys Compd. **408–412**, 1161–1164 (2006). https://doi.org/10.1016/j.jallcom.2004.12.135
42. Shimonosono, T., Hirata, Y., Sameshima, S., Horita, T.: Electronic conductivity of La-doped ceria ceramics. J. Am. Ceram. Soc. **88**, 2114–2120 (2005). https://doi.org/10.1111/j.1551-2916.2005.00401.x
43. Liu, N., Shi, M., Wang, C., Yuan, Y.P., Majewski, P., Aldinger, F.: Microstructure and ionic conductivity of Sr- and Mg-doped $LaGaO_3$. J. Mater. Sci. **41**, 4205–4213 (2006). https://doi.org/10.1007/s10853-006-6309-1
44. Ramesh, S., Raju, K.C.J.: Preparation and characterization of $Ce_{1-x}(Gd_{0.5}Pr_{0.5})_xO_2$ electrolyte for IT-SOFCs. Int. J. Hydrogen Energy **37**, 10311–10317 (2012). https://doi.org/10.1016/j.ijhydene.2012.04.008
45. Huang, J., Gao, Z., Mao, Z.: Effects of salt composition on the electrical properties of samaria-doped ceria/carbonate composite electrolytes for low-temperature SOFCs. Int. J. Hydrogen Energy **35**, 4270–4275 (2010). https://doi.org/10.1016/j.ijhydene.2010.01.063
46. Zhu, B., Liu, X., Zhu, Z., Ljungberg, R.: Solid oxide fuel cell (SOFC) using industrial grade mixed rare-earth oxide electrolytes. Int. J. Hydrogen Energy **33**, 3385–3392 (2008). https://doi.org/10.1016/j.ijhydene.2008.03.065
47. Leng, Y., Chan, S.H., Liu, Q.: Development of LSCF-GDC composite cathodes for low-temperature solid oxide fuel cells with thin film GDC electrolyte. Int. J. Hydrogen Energy **33**, 3808–3817 (2008). https://doi.org/10.1016/j.ijhydene.2008.04.034
48. Ferreira, A.S.V., Soares, C.M.C., Figueiredo, F.M.H.L.R., Marques, F.M.B.: Intrinsic and extrinsic compositional effects in ceria/carbonate composite electrolytes for fuel cells. Int. J. Hydrogen Energy **36**, 3704–3711 (2011). https://doi.org/10.1016/j.ijhydene.2010.12.025
49. Francis, J.S.C., Cologna, M., Montinaro, D., Raj, R.: Flash sintering of anode-electrolyte multilayers for SOFC applications. J. Am. Ceram. Soc. **96**, 1352–1354 (2013). https://doi.org/10.1111/jace.12330
50. Zhou, X., Zhou, F.: Application of La0.3Sr0.7Fe0.7Ti0.3O3-δ/GDC electrolyte in LT-SOFC. Int. J. Hydrogen Energy (2020). https://doi.org/10.1016/j.ijhydene.2020.01.171
51. Marina, O.A., Pederson, L.R., Williams, M.C., Coffey, G.W., Meinhard, K.D., Nguyen, C.D., Thomsen, E.C.: Electrode performance in reversible solid oxide fuel cells. J. Electrochem. Soc. **154**, B452 (2007). https://doi.org/10.1149/1.2710209
52. Lee, K.T., Yoon, H.S., Wachsman, E.D.: The evolution of low temperature solid oxide fuel cells. J. Mater. Res. **27**, 2063–2078 (2012). https://doi.org/10.1557/jmr.2012.194

53. Cowin, P.I., Petit, C.T.G., Lan, R., Irvine, J.T.S., Tao, S.: Recent progress in the development of anode materials for solid oxide fuel cells. Adv. Energy Mater. **1**, 314–332 (2011). https://doi.org/10.1002/aenm.201100108
54. Bastidas, D.M., Tao, S., Irvine, J.T.S.: A symmetrical solid oxide fuel cell demonstrating redox stable perovskite electrodes. J. Mater. Chem. **16**, 1603–1605 (2006). https://doi.org/10.1039/b600532b
55. Liu, Y., Jia, L., Li, J., Chi, B., Pu, J., Li, J.: High-performance Ni in-situ exsolved $Ba(Ce_{0.9}Y_{0.1})_{0.8}Ni_{0.2}O_{3-\delta}/Gd_{0.1}Ce_{0.9}O_{1.95}$ composite anode for SOFC with long-term stability in methane fuel. Compos. Part B Eng. **193**, 108033 (2020). https://doi.org/10.1016/j.compositesb.2020.108033
56. Lu, Z.G., Zhu, J.H., Bi, Z.H., Lu, X.C.: A Co-Fe alloy as alternative anode for solid oxide fuel cell. J. Power Sources **180**, 172–175 (2008). https://doi.org/10.1016/j.jpowsour.2008.02.051
57. Wei, T., Ji, Y., Meng, X., Zhang, Y.: Sr_2NiMoO_6 as anode material for $LaGaO_3$-based solid oxide fuel cell. Electrochem. commun. **10**, 1369–1372 (2008). https://doi.org/10.1016/j.elecom.2008.07.005
58. Mumtaz, S., Ahmad, M.A., Raza, R., Khan, M.A., Ashiq, M.N., Abbas, G.: Nanostructured anode materials for low temperature solid oxide fuel cells: Synthesis and electrochemical characterizations. Ceram. Int. **45**, 21688–21697 (2019). https://doi.org/10.1016/j.ceramint.2019.07.169
59. Benamira, M., Thommy, L., Moser, F., Joubert, O., Caldes, M.T.: New anode materials for IT-SOFC derived from the electrolyte $BaIn_{0.3}Ti_{0.7}O_{2.85}$ by lanthanum and manganese doping. Solid State Ionics **265**, 38–45 (2014). https://doi.org/10.1016/j.ssi.2014.07.006
60. Moura, C.G., Paulo, J., Grilo, D.F., Maribondo, R.: A brief review on anode materials and reactions mechanism in solid oxide fuel cells. Front. Ceram. Sci. **9**, 26–41 (2017). https://doi.org/10.2174/9781681084312117010007
61. Chavan, A.U., Jadhav, L.D., Jamale, A.P., Patil, S.P., Bhosalem, C.H., Bharadwaj, S.R., Patil, P.S.: Effect of variation of NiO on properties of NiO/GDC (gadolinium doped ceria) nano-composites. Ceram. Int. **38**, 3191–3196 (2012). https://doi.org/10.1016/j.ceramint.2011.12.023
62. Fu, C., Chan, S.H., Liu, Q., Ge, X., Pasciak, G.: Fabrication and evaluation of Ni-GDC composite anode prepared by aqueous-based tape casting method for low-temperature solid oxide fuel cell. Int. J. Hydrogen Energy **35**, 301–307 (2010). https://doi.org/10.1016/j.ijhydene.2009.09.101
63. Gil, V., Moure, C., Tartaj, J.: Sinterability, microstructures and electrical properties of Ni/Gd-doped ceria cermets used as anode materials for SOFCs. J. Eur. Ceram. Soc. **27**, 4205–4209 (2007). https://doi.org/10.1016/j.jeurceramsoc.2007.02.119
64. Chen, J.C., Hwang, B.H.: Microstructure and properties of the Ni-CGO composite anodes prepared by the electrostatic-assisted ultrasonic spray pyrolysis method. J. Am. Ceram. Soc. **91**, 97–102 (2008). https://doi.org/10.1111/j.1551-2916.2007.02109.x
65. Ding, C., Lin, H., Sato, K., Hashida, T.: Synthesis of NiO-$Ce_{0.9}Gd_{0.1}O_{1.95}$ nanocomposite powders for low-temperature solid oxide fuel cell anodes by co-precipitation. Scr. Mater. **60**, 254–256 (2009). https://doi.org/10.1016/j.scriptamat.2008.10.020
66. Lay, E., Gauthier, G., Rosini, S., Savaniu, C., Irvine, J.T.S.: Ce-substituted LSCM as new anode material for SOFC operating in dry methane. Solid State Ionics **179**, 1562–1566 (2008). https://doi.org/10.1016/j.ssi.2007.12.072
67. Sinha, A., Miller, D.N., Irvine, J.T.S.: Development of novel anode material for intermediate temperature SOFC (IT-SOFC). J. Mater. Chem. A **4**, 11117–11123 (2016). https://doi.org/10.1039/c6ta03404g
68. Rossmeisl, J., Bessler, W.G.: Trends in catalytic activity for SOFC anode materials. Solid State Ionics **178**, 1694–1700 (2008). https://doi.org/10.1016/j.ssi.2007.10.016
69. Yang, X., Chen, J., Panthi, D., Niu, B., Lei, L., Yuan, Z., Du, Y., Li, Y., Chen, F., He, T.: Electron doping of $Sr_2FeMoO_{6-\delta}$ as high performance anode materials for solid oxide fuel cells. J. Mater. Chem. A **7**, 733–743 (2019). https://doi.org/10.1039/c8ta10061f
70. Giannici, F., Gregori, G., Longo, A., Chiara, A., Maier, J., Martorana, A.: X-ray absorption under operating conditions for solid oxide fuel cells electrocatalysts: the case of LSCF/YSZ. Surfaces **2**, 32–40 (2019). https://doi.org/10.3390/surfaces2010003
71. Verbraeken, M.C., Iwanschitz, B., Mai, A., Irvine, J.T.S.: Evaluation of Ca doped $La_{0.2}Sr_{0.7}TiO_3$ as an alternative material for use in SOFC anodes. J. Electrochem. Soc. **159**, 757–762 (2012). https://doi.org/10.1149/2.001212jes
72. Steiger, P., Burnat, D., Madi, H., Mai, A., Holzer, L., Herle, J.V., Krocher, O., Heel, A., Ferri, D.: Sulfur poisoning recovery on a solid oxide fuel cell anode material through reversible segregation of Nickel. Chem. Mater. **31**, 748–758 (2019). https://doi.org/10.1021/acs.chemmater.8b03669
73. Zha, S., Cheng, Z., Liu, M.: A sulfur-tolerant anode material for SOFCs $Gd_2Ti_{1.4}Mo_{0.6}O_7$. Electrochem. solid-state Lett. **8**, 406–408 (2005). https://doi.org/10.1149/1.1945370
74. Li, F., Zhang, J., Luan, J., Liu, Y., Han, J.: Preparation of Bi_2O_3-doped NiO/YSZ anode materials for SOFCs. Surf. Rev. Lett. **24**, 1750092 (2017). https://doi.org/10.1142/s0218625x17500925
75. Dong, G., Yang, C., He, F., Jiang, Y., Ren, C., Gan, Y., Lee, M., Xue, X.: Tin doped $PrBaFe_2O_{5+\delta}$ anode material for solid oxide fuel cells. RSC Adv. **7**, 22649–22661 (2017). https://doi.org/10.1039/c7ra03143b
76. Shaheen, K., Shah, Z., Gulab, H., Hanif, M.B., Faisal, S., Suo, H.: Metal oxide nanocomposites as anode and cathode for low temperature solid oxide fuel cell. Solid State Sci. **102**, 106162 (2020). https://doi.org/10.1016/j.solidstatesciences.2020.106162
77. Istomin, S.Y., Antipov, E.V.: Cathode materials based on perovskite-like transition metal oxides for intermediate temperature solid oxide fuel cells. Russ. Chem. Rev. **82**, 686–700 (2013). https://doi.org/10.1070/rc2013v082n07abeh004390
78. Haverkort, M.W., Hu, Z., Cezar, J.C., Burnus, T., Hartmann, H., Reuther, M., Zobel, C., Loernz, T., Tanaka, A., Brookes, N.B., Hsieh, H.H., Lin, H.J., Chen, C.T., Tjeng, L.H.: Spin state transition in $LaCoO_3$ studied using soft X-ray absorption spectroscopy and magnetic circular dichroism. Phys. Rev. Lett. **97**, 38–41 (2006). https://doi.org/10.1103/PhysRevLett.97.176405
79. H. Yokokawa, "Overview of intermediate-temperature solid oxide fuel cells," *T. Ishihara (ed.), Perovskite Oxide Solid Oxide Fuel Cells*, vol. New York:, 2009, doi: https://doi.org/10.1007/978-0-387-77708-5.
80. Sun, J., Liu, X., Han, F., Zhu, L., Bi, H., Wang, H., Yu, S., Pei, L.: $NdBa_{1-x}Co_2O_{5+\delta}$ as cathode materials for IT-SOFC. Solid State Ionics **288**, 54–60 (2016). https://doi.org/10.1016/j.ssi.2015.12.023
81. Choi, S., Yoo, S., Kim, J., Park, S., Jun, A., Sengodan, S., Kim, J., Shin, J., Jeong, H.Y., Choi, Y., Kim, G., Liu, M.: Highly efficient and robust cathode materials for low-temperature solid oxide fuel cells: $PrB\alpha_{0.5}Sr_{0.5}Co_{2-x}Fe_xO_{5+\delta}$. Sci. Rep. **3**, 3–8 (2013). https://doi.org/10.1038/srep02426
82. Ma, J., Tao, Z., Kou, H., Fronzi, M., Bi, L.: Evaluating the effect of Pr-doping on the performance of strontium-doped lanthanum ferrite cathodes for protonic SOFCs. Ceram. Int. **46**, 4000–4005 (2020). https://doi.org/10.1016/j.ceramint.2019.10.017
83. Dai, H., Kou, H., Tao, Z., Liu, K., Xue, M., Zhang, Q., Bi, L.: Optimization of sintering temperature for SOFCs by a

co-firing method. Ceram. Int. **46**, 6987–6990 (2020). https://doi.org/10.1016/j.ceramint.2019.11.134
84. Baumann, F.S., Fleig, J., Cristiani, G., Stuhlhofer, B., Habermeier, H.-U., Maier, J.: Quantitative comparison of mixed conducting SOFC cathode materials by means of thin film model electrodes. J. Electrochem. Soc. **154**, B931–B941 (2007). https://doi.org/10.1149/1.2752974
85. Kim, J., Sengodan, S., Kwon, G., Ding, D., Shin, J., Liu, M., Kim, G.: Triple-conducting layered perovskites as cathode materials for proton-conducting solid oxide fuel cells. Chemsuschem **7**, 2811–2815 (2014). https://doi.org/10.1002/cssc.201402351
86. Wang, B., Bi, L., Zhao, X.S.: Liquid-phase synthesis of $SrCo_{0.9}Nb_{0.1}O_{3-\delta}$ cathode material for proton-conducting solid oxide fuel cells. Ceram. Int. **44**, 5139–5144 (2018). https://doi.org/10.1016/j.ceramint.2017.12.116
87. Baharuddin, N.A., Muchtar, A., Somalu, M.R.: Short review on cobalt-free cathodes for solid oxide fuel cells. Int. J. Hydrogen Energy **42**, 9149–9155 (2017). https://doi.org/10.1016/j.ijhydene.2016.04.097
88. Ding, H., Xue, X.: Cobalt-free layered perovskite $GdBaFe_2O_{5+x}$ as a novel cathode for intermediate temperature solid oxide fuel cells. J. Power Sources **195**, 4718–4721 (2010). https://doi.org/10.1016/j.jpowsour.2010.02.027
89. Lee, S.J., Yong, S.M., Kim, D.S., Kim, D.K.: Cobalt-free composite cathode for SOFCs: Brownmillerite-type calcium ferrite and gadolinium-doped ceria. Int. J. Hydrogen Energy **37**, 17217–17224 (2012). https://doi.org/10.1016/j.ijhydene.2012.08.100
90. Zhou, Q., Zhang, L., He, T.: Cobalt-free cathode material $SrFe_{0.9}Nb_{0.1}O_{3-\delta}$ for intermediate-temperature solid oxide fuel cells. Electrochem. commun. **12**, 285–287 (2010). https://doi.org/10.1016/j.elecom.2009.12.016
91. Jiang, S., Zhou, W., Niu, Y., Zhu, Z., Shao, Z.: Phase transition of a cobalt-free perovskite as a high-performance cathode for intermediate-temperature solid oxide fuel cells. Chemsuschem **5**, 2023–2031 (2012). https://doi.org/10.1002/cssc.201200264
92. X. Yu, W. Long, F. Jin, and T. He, Cobalt-free perovskite cathode materials $SrFe_{1-x}Ti_xO_{3-\delta}$ and performance optimization for intermediate-temperature solid oxide fuel cells, vol. 123. Elsevier Ltd, 2014.
93. Ling, Y., Zhao, L., Lin, B., Dong, Y., Zhang, X., Meng, G., Liu, X.: Investigation of cobalt-free cathode material $Sm_{0.5}Sr_{0.5}Fe_{0.8}Cu_{0.2}O_{3-\delta}$ for intermediate temperature solid oxide fuel cell. Int. J. Hydrogen Energy **35**, 6905–6910 (2010). https://doi.org/10.1016/j.ijhydene.2010.04.021
94. Zhu, Z., Yan, L., Sun, W., Liu, H., Liu, T., Liu, W.: A cobalt-free composite cathode prepared by a superior method for intermediate temperature solid oxide fuel cells. J. Power Sources **217**, 431–436 (2012). https://doi.org/10.1016/j.jpowsour.2012.06.049
95. Duan, C., Hook, D., Chen, Y., Tong, J., O'Hayre, R.: Zr and Y co-doped perovskite as a stable, high performance cathode for solid oxide fuel cells operating below 500°C. Energy Environ. Sci. **10**, 176–182 (2017). https://doi.org/10.1039/c6ee01915c
96. Zhang, Z., Zhu, Y., Zhong, Y., Zhou, W., Shao, Z.: Anion doping: A new strategy for developing high-performance perovskite-type cathode materials of solid oxide fuel cells. Adv. Energy Mater. **7**, 1–9 (2017). https://doi.org/10.1002/aenm.201700242
97. Li, M., Zhao, M., Li, F., Zhao, W., Peterson, V.K., Xu, X., Shao, Z., Gentle, I., Zhu, Z.: A niobium and tantalum co-doped perovskite cathode for solid oxide fuel cells operating below 500°c. Nat. Commun. **8**, 1–9 (2017). https://doi.org/10.1038/ncomms13990
98. Zhou, W., Sunarso, J., Zhao, M., Liang, F., Klande, T., Feldhoff, A.: A highly active perovskite electrode for the oxygen reduction reaction below 600°c. Angew. Chemie - Int. Ed. **52**, 14036–14040 (2013). https://doi.org/10.1002/anie.201307305
99. Hussain, M., Muneer, M., Abbas, G., Shakir, I., Iqbal, A., Javed, M.A., Iqbal, M., Ur Rehman, Z., Raza, R.: Cobalt free LaxSr1-xFe1-yCuyO3-δ (x= 0.54, 0.8, y = 0.2, 0.4) perovskite structured cathode for SOFC. Ceram. Int. **46**, 18208–18215 (2020). https://doi.org/10.1016/j.ceramint.2020.04.143
100. Salvatore Arico, A., Bruce, P., Scrosati, B., Tarascon, J.M., Van Schalkwijk, W.: A siloxane-incorporated copolymer as an in situ cross-linkable binder for high performance silicon anodes in Li-ion batteries. Nat. Mater. **4**, 366–377 (2005). https://doi.org/10.1039/c6nr01559j
101. Yuan, Q., Duan, H.H., Le Li, L., Sun, L.D., Zhang, Y.W., Yan, C.H.: Controlled synthesis and assembly of ceria-based nanomaterials. J. Colloid Interface Sci. **335**, 151–167 (2009). https://doi.org/10.1016/j.jcis.2009.04.007
102. Dong, Y., Hampshire, S., Zhou, J.E., Meng, G.: Synthesis and sintering of Gd-doped CeO_2 electrolytes with and without 1 at.% CuO dopping for solid oxide fuel cell applications. Int. J. Hydrogen Energy **36**, 5054–5066 (2011). https://doi.org/10.1016/j.ijhydene.2011.01.030
103. Bellino, M.G., Sacanell, J.G., Lamas, D.G., Leyva, A.G., Walsöe De Reca, N.E.: High-performance solid-oxide fuel cell cathodes based on cobaltite nanotubes. J. Am. Chem. Soc. **129**, 3066–3067 (2007). https://doi.org/10.1021/ja068115b
104. Martinelli, H., Lamas, D.G., Leyva, A.G., Sacanell, J.: Influence of particle size and agglomeration in solid oxide fuel cell cathodes using manganite nanoparticles. Mater. Rsearch Expresss **5**, 075013–075025 (2018)
105. Zhi, M., Lee, S., Miller, N., Menzler, N.H., Wu, N.: An intermediate-temperature solid oxide fuel cell with electrospun nanofiber cathode. Energy Environ. Sci. **5**, 7066–7071 (2012). https://doi.org/10.1039/c2ee02619h
106. Ishihara, T.: Nanomaterials for advanced electrode of low temperature solid oxide fuel cells (SOFCs). J. Korean Ceram. Soc. **53**, 469–477 (2016). https://doi.org/10.4191/kcers.2016.53.5.469
107. Yoon, J., Cho, S., Kim, J.H., Lee, J.-H., Bi, Z., Serquis, A., Zhang, X., Manthiram, A., Wang, H.: Vertically aligned nanocomposite thin films as a cathode/electrolyte interface layer for thin-film solid oxide fuel cells. Adv. Funct. Mater. **19**, 3868–3873 (2009). https://doi.org/10.1002/adfm.200901338
108. Evans, A., Benal, C., Darbandi, A.J., Hahn, H., Martynczuk, J., Gauckler, L.J., Prestat, M.: Integration of spin-coated nanoparticulate-based $La_{0.6}Sr_{0.4}CoO_{3-\delta}$ cathodes into micro-solid oxide fuel cell membranes. Fuel Cells **13**, 441–444 (2013). https://doi.org/10.1002/fuce.201300020
109. Guan, Y., Li, W., Gong, Y., Liu, G., Zhang, X., Chen, J., Gelb, J., Yun, W., Xiong, Y., Tian, Y., Wang, H.: Analysis of the three-dimensional microstructure of a solid-oxide fuel cell anode using nano X-ray tomography. J. Power Sources **196**, 1915–1919 (2011). https://doi.org/10.1016/j.jpowsour.2010.09.059
110. Boldrin, P., Trejo, E.R., Yu, J., Gruar, R.I., Tighe, C.J., Chang, K.C., Ilavsky, J., Darr, J.A., Brandon, N.: Nanoparticle scaffolds for syngas-fed solid oxide fuel cells. J. Mater. Chem. A **3**, 3011–3018 (2015). https://doi.org/10.1039/c4ta06029f
111. Pelegrini, L., Neto, J.B.R., Hotza, D.: Process and materials improvements on Ni/Cu-YSZ composites towards nanostructured SOFC anodes: a review. Rev. Adv. Mater. Sci. **46**, 6–21 (2016)
112. Kwon, O., Kim, K., Joo, S., Jeong, H.Y., Shin, J., Han, J.W., Sengodan, S., Kim, G.: Self-assembled alloy nanoparticles in a layered double perovskite as a fuel oxidation catalyst for solid oxide fuel cells. J. Mater. Chem. A **6**, 15947–15953 (2018). https://doi.org/10.1039/c8ta05105d
113. Cavallaro, A., Pramana, S.S., Trejo, E.R., Sherrel, P.C., Ware, E., Kilner, J.A., Skinner, S.J.: Amorphous-cathode-route towards low temperature SOFC. Sustain. Energy Fuels **2**, 862–875 (2018). https://doi.org/10.1039/c7se00606c